Journal of Colloid and Interface Science 354 (2011) 858–865

Contents lists available at ScienceDirect

Journal of Colloid and Interface Science

www.elsevier.com/locate/jcis

Preparation and characterization of ultrathin dual-layer ionic liquid lubrication film assembled on silica surfaces

Jibin Pu [a,b], Liping Wang [a,*], Yufei Mo [c], Qunji Xue [a]

[a] State Key Laboratory of Solid Lubrication, Lanzhou Institute of Chemical Physics, Chinese Academy of Science, Lanzhou 730000, China
[b] Graduate School of Chinese Academy of Science, Beijing 100080, China
[c] School of Chemistry & Chemical Engineering, Guangxi University, Nanning 530004, China

ARTICLE INFO

Article history:
Received 20 September 2010
Accepted 2 November 2010
Available online 9 November 2010

Keywords:
Micro/nanotribology
Adhesion
Ionic liquids
SAMs
AFM

ABSTRACT

A novel ultrathin dual-layer film, which contained both bonded and mobile phases in ionic liquids (ILs) layer, was fabricated successfully on a silicon substrate modified by a self-assembled monolayer (SAM). The formation and surface properties of the films were analyzed using ellipsometer, water contact angle meter, attenuated total reflectance Fourier transform infrared spectroscopy, multi-functional X-ray photoelectron spectroscopy, and atomic force microscope. Meanwhile, the adhesive and nanotribological behaviors of the films were evaluated by a homemade colloidal probe. A ball-on-plate tribometer was used to evaluate the microtribological performances of the films. Compared with the single-layer ILs film deposited directly on the silicon surface, the as-prepared dual-layer film shows the improved tribological properties, which is attributed to the special chemical structure and outstanding physical properties of the dual-layer film, i.e., the strong adhesion between bonded phase of ILs and silicon substrate via the chemical bonding with SAM, the interlinked hydrogen bonds among the molecules, and two-phase structure composed of steady bonded phase with load-carrying capacity and flowable mobile phase with self-replenishment property.

1. Introduction

Micro/nano-electromechanical systems (M/NEMS) are expected to have a major impact on our lives due to their superior performances and low cost in many areas such as nanotechnology, high density storage, optical communication, and biomedicine [1–3]. However, on micro/nano-scales, the increased ratio of surface area to volume in M/NEMS devices causes serious adhesion and friction which reduce the performances and the operating lifetimes of M/NEMS devices [4]. To improve mechanical performance, M/NEMS require a protective lubricant coating of low friction and high durability. The ideal lubricant for M/NEMS should possess the following properties: molecularly thick, easy to be applied, chemically bonded to micro/nano-device surfaces, insensitive to environment and high durability [5,6].

Self-assembled monolayers (SAMs), formed typically by the adsorption of alkylsilanes on silicon surfaces [7], have attracted widespread interests in many applications including friction-related fundamental studies due to good anti-rupture performance and uniform chemical adsorbability [8–10]. However, the low molecular mobility has limited SAMs' application, because there are no tribological contributions of the mobile molecules, such as replenishment, low shear strength, trapping among the microasperities [11]. To utilize SAMs as a thin film lubricant, it is necessary to have a mobile characteristic in addition to strong adhesion to substrates [5].

Ionic liquids (ILs), which are composed of bulky and asymmetrical organic cations and evenly shaped inorganic or organic anions, are known as synthetic salts with a melting point below 100 °C [12]. ILs have found wide applications in many ways due to their unique properties such as negligible volatility, nonflammability, high chemical and physical stability, low melting point, high thermal conductivity, controlled miscibility with organic compounds, and recycling [13–15]. As a result, the synthesis, characterization, properties, and applications of ILs have been rapidly grown areas of the interests [13,16–20]. In recent years, as potentially molecular-level lubricant for reducing adhesion and friction in M/NEMS, many researchers have paid considerable attention to desirable tribological properties of ILs [21].

Liu and co-workers reported tribological properties of some ILs, and found that these ILs exhibited excellent friction reducing and antiwear performances for different sliding pairs [22–26]. However, a great number of previous researches on ILs lubricants mainly focused on the fluid lubrication or boundary lubrication under high applied load on macro-scale [27–30]. More recently, a few researches on the tribological properties of ultra-thin ILs films

* Corresponding author. Fax: +86 931 8277088.
E-mail address: lpwang@licp.cas.cn (L. Wang).

0021-9797/$ - see front matter © 2010 Elsevier Inc. All rights reserved.
doi:10.1016/j.jcis.2010.11.001

whose thicknesses were well below a few tens of nanometers have been reported, which aimed at their application in M/NEMS [21,31–33]. For example, our group had investigated micro/nanotribological properties of several kinds of ultra-thin ILs films, and concluded that these ILs were suitable for thin film lubrication and had potential application prospect in magnetic storage systems and M/NEMS [34–38]. However, these ILs films were formed on silicon surfaces by the way of weak physisorption rather than strong chemical bonding. A thin ILs film should basically have both an adhesive nature for protecting the solid substrate surface and a fluidic nature for reducing friction. Based on this view, Bhushan et al. prepared ILs coatings with partially bonded phase on silicon surfaces by heating and investigated their tribological properties [39]. They found that thermally treated coatings with a fraction of mobile lubricant (i.e., partially bonded) were better able to protect the silicon substrates against wear as compared with the fully bonded coatings, and this enhanced protection was attributed to lubricant replenishment. Kato et al. investigated the influence of ratio of bonded perfluorodecyltrichlorosilane (FDTS) to mobile perfluoroalkylpolyether Fomblin Z03 (—CF_3) on tribological behaviors of mixed lubricants and compared them with perfluoroalkylpolyether Fomblin Zdol (—CF_2CH_2OH) lubricants [40], and found that the friction coefficient of a disk coated with mixed lubricants increased linearly with the bonded ratio over a range of about 25–100%, while the friction coefficient of the perfluoroalkylpolyether Fomblin Zdol-coated disk decreased with the bonded ratio. On the other hand, the mixed lubricant showed superior antiwear properties because the perfluorodecyltrichlorosilane network acted as a barrier against the displacement of the mobile perfluoroalkylpolyether Fomblin Z03 molecules. McCabe et al. studied the effect of ILs on the shear dynamics and tribological properties of contacting ordered alkylsilane SAM on SiO_2 surfaces using molecular dynamics simulation [41]. Their simulation results showed that the ILs lubricants reduced the frictional force between the contacting monolayers at a given normal load, because ILs might incorporate into the SAM chains at low normal loads and potentially repair a damaged area of the coating, and restore the tribological properties. To the best of our knowledge, so far there are still no reports about formation of two-phase structure of the thin ILs films via chemical bonding with SAMs for improving their tribological behaviors. In the work, a steady SAM was constructed on a hydroxylated silicon surface, which made it feasible for ILs carrying carboxylic groups to be partially bonded to the silicon substrate by the special chemical reaction. As a result, a two-phase structure of the thin ILs film composed of bonded and mobile fractions, as well as interlinked hydrogen bonds among the molecules, was produced [42–44]. Then the relationship between chemical compositions, microstructure and tribological behaviors of the as-prepared dual-layer film was investigated, aiming to further optimize the micro/nanotribological behaviors of the thin ILs films.

2. Materials and methods

2.1. Materials

3-Aminopropyl-triethoxysilane (99%, APS) was purchased from Aldrich Chemical Co. 1-Carboxyethyl-3-methyl imidazolium hexafluorophosphate ionic liquids (denoted as IL-COOH) was synthesised and purified, the molecular structure is shown in Fig. 1. The as-received acetone, isopropanol, and ethanol were all analytical purity. P-type polished single-crystal silicon (1 0 0) wafers (obtained from GRINM Semiconductor Materials Co., Beijing, China) were used as substrates. Deionized water was used for preparation of all aqueous solutions, and for rinsing.

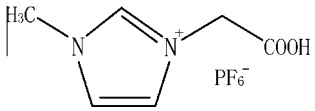

Fig. 1. Molecular structure of 1-carboxyethyl-3-methyl imidazolium hexafluorophosphate ionic liquids.

2.2. Preparation of the dual-layer film

The silicon wafers with dimensions of 10 × 10 × 0.5 mm were ultrasonically cleaned in acetone followed by isopropanol for 5 min, and immersed in freshly prepared Piranha solution (a mixture of 7:3 (v/v) 98% H_2SO_4 and 30% H_2O_2) at 90 °C for 30 min to get hydroxyl-terminated surfaces. Then the silicon wafers were rinsed thoroughly with deionized water, flushed with a stream of ultrapure nitrogen gas, and placed into the fresh 5 mM solution of APS in mixed solvent of acetone and ultrapure water (the volume ratio of acetone and water was 5:1) for 12 h. Thus the APS molecules were assembled on the hydroxylated silicon surfaces by forming stable Si—O—Si covalent bonds [9]. After being sonicated in acetone for 5 min to remove the physically adsorbed APS molecules, the APS-assembled silicon wafers were dipped into a 0.2% (w/v) dilute solution of IL-COOH in acetone for 3 min and withdrew from the solution at a constant velocity of 60 μm/s. Then, these films were heated at 140 °C in nitrogen flow for 30 min to accelerate the acid-amide reaction between IL-COOH and APS, and cooled in a desiccator. In this way, a desired two-phase structure composed of bonded and unbonded IL-COOH molecules was produced on silicon surface. Lastly, some samples of the developed dual-layer films with two-phase structure in IL-COOH layer were ultrasonically cleaned in acetone to remove the unbonded IL-COOH molecules for subsequent XPS and ATR-FTIR measurements. For comparison, the single-layer IL-COOH film was dip-coated on the hydroxylated silicon surface without the deposition of APS. All procedures mentioned above were carried out in a class-100 clean room at 20 °C and a humidity of 17%.

2.3. Characterization of the thin films

The static water contact angles on the thin films were determined using a DSA100 contact angle meter (Kruss, Germany). The volume of water droplets used for the measurement was about 5 μL. At least three replicable measurements were carried out at different points for each specimen, and the measurement error was below 2°. The thicknesses of thin films were measured using a L116E ellipsometer equipped with a He–Ne laser source (632.8 nm) at an incident angle of 50° (Gaertner, USA). Five replicable measurements were carried out for each specimen to get the averages. The real reflective indices of 1.46, 1.42 and 1.41 were set for the silicon oxide, APS and IL-COOH on the silicon surfaces, respectively. Attenuated total reflectance Fourier transform infrared (ATR-FTIR) spectra of the thin films were recorded by a Harrick horizontally Ge-attenuated total reflection accessory (GATR, incident angle of 65°) attached to an IFS 66V/S Fourier transformation infrared spectrometer (Bruker, Germany). The spectra were collected for 64 scans at a resolution of 4 cm^{-1} and the background was collected in the absence of the specimens. To eliminate the interference of H_2O and CO_2, both the sample chamber and the optical chamber were evacuated to 3 mbar. Chemical compositions and element chemical state on the specimen surfaces were also analyzed on a PHI-5702 multi-functional X-ray photoelectron spectrometer (XPS, Perkin–Elmer, USA) with an excitation source of Mg Kα radiation ($h\upsilon$ = 1253.6 eV) at take-off angle of 35°, and the vacuum degree of chamber was about 5×10^{-8} Torr during testing. The binding energies of the target elements were determined at a pass energy of 29.35 eV with a resolution of about

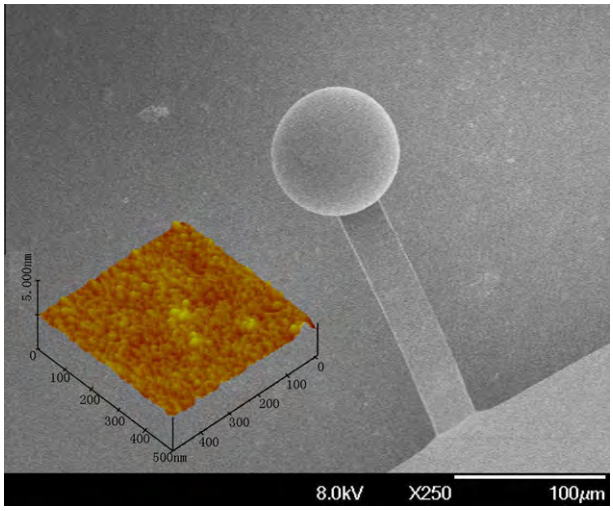

Fig. 2. SEM image of the colloid probe and AFM topography of microsphere.

±0.3 eV, the binding energy of contaminated carbon (C1s 284.8 eV) was used as reference. A nanoscope IIIa multimode atomic force microscope (AFM, Veeco, USA) was employed to observe the surface morphologies of the thin films in tapping mode.

2.4. Tribological properties of the thin films

The nanotribological properties of the thin films were studied using a CSPM 4000 AFM (Being Nano-Instruments, China) in contact mode. A colloidal probe (normal force constant 2 N/m) was prepared by gluing borosilicate glass microsphere with a radius of 28 μm onto a tipless cantilever for nanotribological measurements. Scanning electron microscope (SEM) image of the colloidal probe and the three-dimensional AFM topography of microsphere are shown in Fig. 2. No attempt was made to calibrate the torsional force constant of the colloidal probe. The output voltages were directly used as relative friction force. A series of friction–load curves were obtained in linear loading process, and each curve represented an average over five separate measurement locations. The same colloidal probe was used to obtain the adhesive behaviors of the thin films. The pull-off force was reckoned as the adhesive force, which was given by $F_{Adhesion} = K_c Z_p$, where K_c is the force constant of the colloidal probe and Z_p is the vertical displacement of the piezotube, i.e., the deflection of the colloidal probe resulting from adhesion. Furthermore, to avoid the influence of molecules which might transfer to microsphere surface, the colloidal probe was scanned on cleaved mica surface to remove physically adsorbed molecules before each test. All of above experiments were carried out at 18 °C and a relative humidity of 15%.

Microtribological tests were carried out on a UMT-2MT tribometer (CETR, USA) in a ball-on-plate reciprocating mode. Commercially availed AISI-52100 steel balls with a diameter of 3.18 mm and a RMS roughness of about 8.2 nm were used as the stationary upper counterparts, while the lower specimens were mounted onto a reciprocating table with a traveling distance of 5 mm. Prior to the test, the steel ball was cleaned with acetone-soaked cotton. Friction coefficient versus sliding time curves were recorded automatically, and the measurements were performed three times for each test condition. It was assumed that lubrication failure of the thin films occurred as the friction coefficient rose sharply to a high and stable value being similar to that of a cleaned silicon oxide against the same counterpart (about 0.65), and the sliding time was recorded as the antiwear life of the thin films. The wear scar morphologies of the thin films were observed with MicroXAM 3D non-contact interferometric microscope with phase mode (ADE, USA). All tests were conducted at 20 °C and a relative humidity of 10%.

3. Results and discussion

3.1. Characterization of the thin films

The construction process of a novel ultrathin dual-layer film containing both bonded and mobile ILs phases on the silicon substrate modified by APS-SAM is shown schematically in Fig. 3. APS was first introduced onto the silicon surface as an anchor layer [9], then the incoming IL-COOH molecules were incompletely chemically grafted to the amino-terminated silicon surface to obtain the bonded phase. The water contact angles on the hydroxylated silicon surface and various films, along with their thicknesses and RMS roughness, are listed in Table 1. The measured thickness of APS is about 0.8 nm, which matches well with the projection of an all-trans extended molecular chain of APS self-assembled on the silicon surface [45]. Thus it can be inferred that a high-quality APS monolayer has been formed on the hydroxylated silicon surface. The water contact angle on APS-SAM is about 44°, which is within the range of contact angles on amino-terminated SAMs reported [46,47]. Because a high contact angle of APS-SAM generally corresponds to a disorder structure with more exposure of the alkyl chains [48], it can be deduced that the prepared APS-SAM is well organized and most likely terminated with amino groups. After being dipped into the solution of IL-COOH in acetone for 3 min, an IL-COOH layer of 3.1 nm was deposited atop APS-SAM, which was designated as APSIL-untreated. The water contact angle of APSIL-untreated film is 17°, quite close to the value of IL-COOH film deposited directly on hydroxylated silicon surface, which confirms the presence of IL-COOH layer on APS-SAM. When APSIL-untreated film was heated at 140 °C for 30 min, which was designated as APSIL, the thickness of IL-COOH layer and its water contact angle sep-

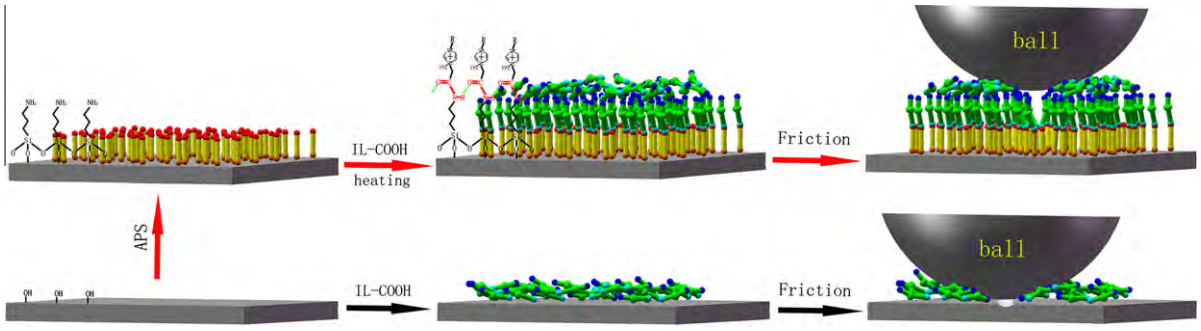

Fig. 3. Schematic drawing of the constructing process and frictional mechanism of APSIL film and IL-COOH film.

Table 1
Water contact angle, thickness and RMS roughness for the various surfaces.

Test samples	Water contact angle (°)	Thickness (nm)	RMS (nm)
SiO_2/Si	<5	3.1	0.1
APS-SAM	48	0.8	0.2
IL-COOH	15	3.5	0.6
APSIL-untreated	17	3.1[a]	0.5
APSIL	28	2.2[a]	0.4
APSIL-wash	51	0.9[a]	0.2

[a] 3.1 nm, 2.2 nm and 0.9 nm were all the thicknesses of the ionic liquids layers.

arately varied to 2.2 nm and 28°, which indicated that the partial bonding and leveling off process occurred. Then the APSIL film was fully washed in acetone to removed unbonded IL-COOH molecules, which was designated as APSIL-wash. As a result, the thickness of IL-COOH layer (namely bonded IL-COOH) reduced to 0.9 nm, and the water contact angle increased to 51° due to exposure of non-polar substituted alkyl chains of the orderly bonded IL-COOH molecules [49,50]. The ratio of bonded phase to mobile phase in ILs layer, namely the bonded ratio, is defined as follows [40]:

$$\text{Bonded ratio } (\%) = \frac{\text{thickness of bonded IL-COOH}}{\text{total film thickness}} \times 100.$$

In the present work, the bonded ratio of IL-COOH is 29% according to above computational method.

ATR-FTIR spectra of the thin films in the frequency range of 3250–1250 cm^{-1} are shown in Fig. 4. For APS-SAM film, the asymmetric and symmetric methylene vibration peaks separately appear at 2925 cm^{-1} and 2854 cm^{-1}. The peaks at 1573 cm^{-1} and 1465 cm^{-1} are assigned to the deformation vibration of N—H and C—H bond, respectively. The stretching vibration peak of the C—N bond appears at 1367 cm^{-1}. For APSIL-wash film, the presence of the characteristic absorption peaks at 1647 cm^{-1} and 1542 cm^{-1}, arising from amide I bond (predominantly C═O stretching) and amide II bond (involving torsional motion of both N—H and C—N), is a visible evidence of the chemical reaction between APS and IL-COOH forming the covalent amide bond (—NHC═O), which is well supported by numerous literature reports [42,51–53]. Moreover, due to the existence of the hydrogen bonds which can induce a decrease in the electron density of the C═O bond and an increasing restriction in N—H bending, the red shift of amide I absorption band and the blue shift of amide II absorption band are observed as compared with non-hydrogen-bonded state at around 1690 cm^{-1} and 1510 cm^{-1}, which is in agreement with Whitesides's report about the existence of hydrogen bonds in the SAMs based on the FTIR spectrum in which the amide I and the amide II are located respectively at 1639–1650 cm^{-1} and 1542–1550 cm^{-1} [42,51].

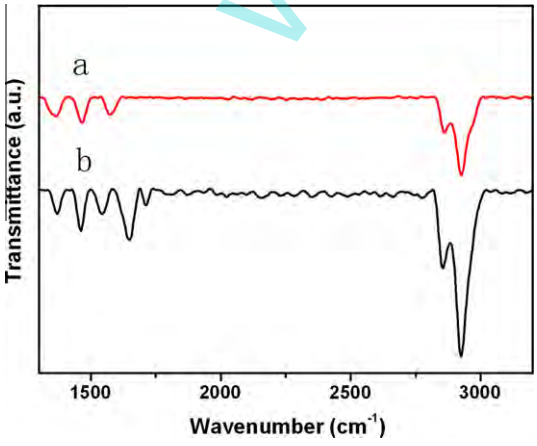

Fig. 4. ATR-FTIR spectra of the thin films: (a) APS-SAM and (b) APSIL-wash.

In order to further characterize the interaction between APS and IL-COOH, XPS data of APSIL-wash film was recorded. Appearance of fluorine (F1s) and phosphorus (P2s, P2p) in the full scan survey spectrum, as shown in Fig. 5a, indicates that IL-COOH is coated successfully on APS-SAM. The fine spectra of carbon (C1s) and nitrogen (N1s) are shown in Fig. 5b and c, respectively. There are three peaks arising from C1s spectrum. The first peak at 284.8 eV can be assigned to the CH_2 groups. The second peak at 286.7 eV might originate from the C atoms bonded to the N atoms (O═C—N—C*) [54], namely C atoms in amide I bonds, while the

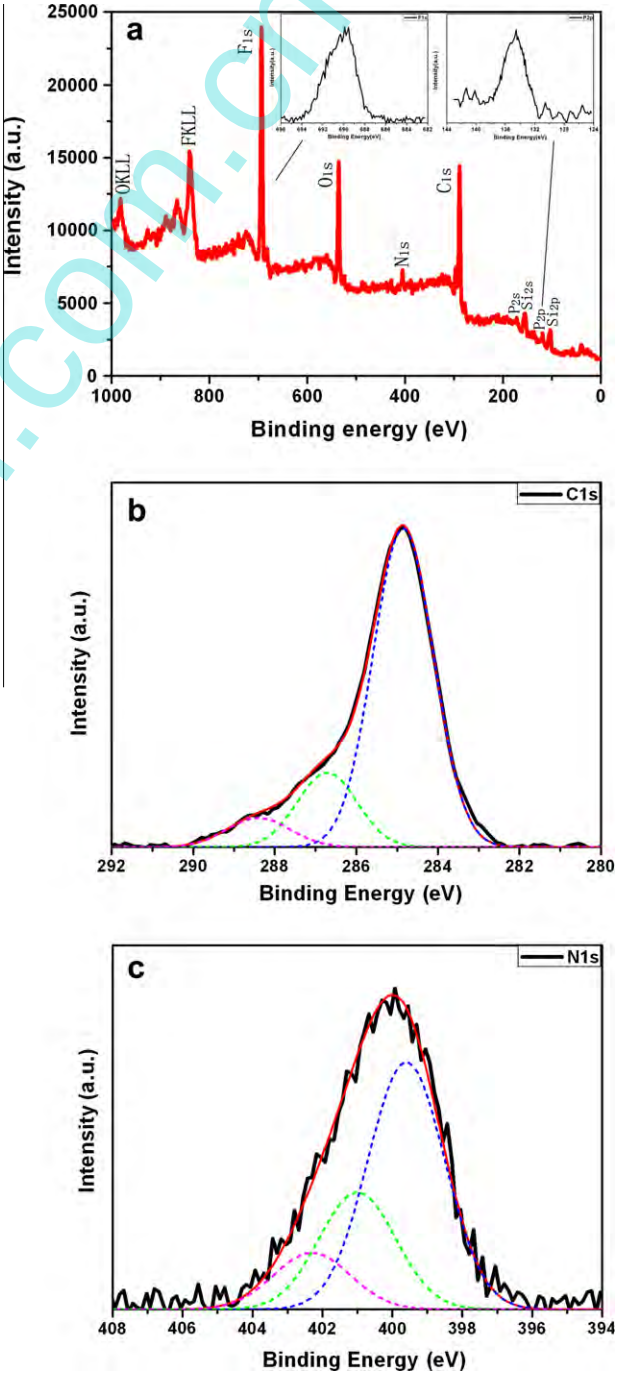

Fig. 5. XPS spectra of APSIL-wash film: (a) full scan survey spectrum and fine survey spectra of F1s and P2p; (b) C1s spectrum; (c) N1s spectrum.

third peak at 288.3 eV can be attributed to the amide-C (O═C*—N—C) [54]. The fitting results clearly confirm the existence of chemical bond between APS and IL-COOH, that is to say, a bonded phase of IL-COOH is formed on APS-SAM. The N1s spectrum further supports this conclusion. While the peak at 399.6 eV is assigned to the N atoms in the amino groups, the peak appearing at 400.8 eV can be attributed to the amide-N (O═C—N*) [54,55]. The electron withdrawing effect of carbonyl groups results

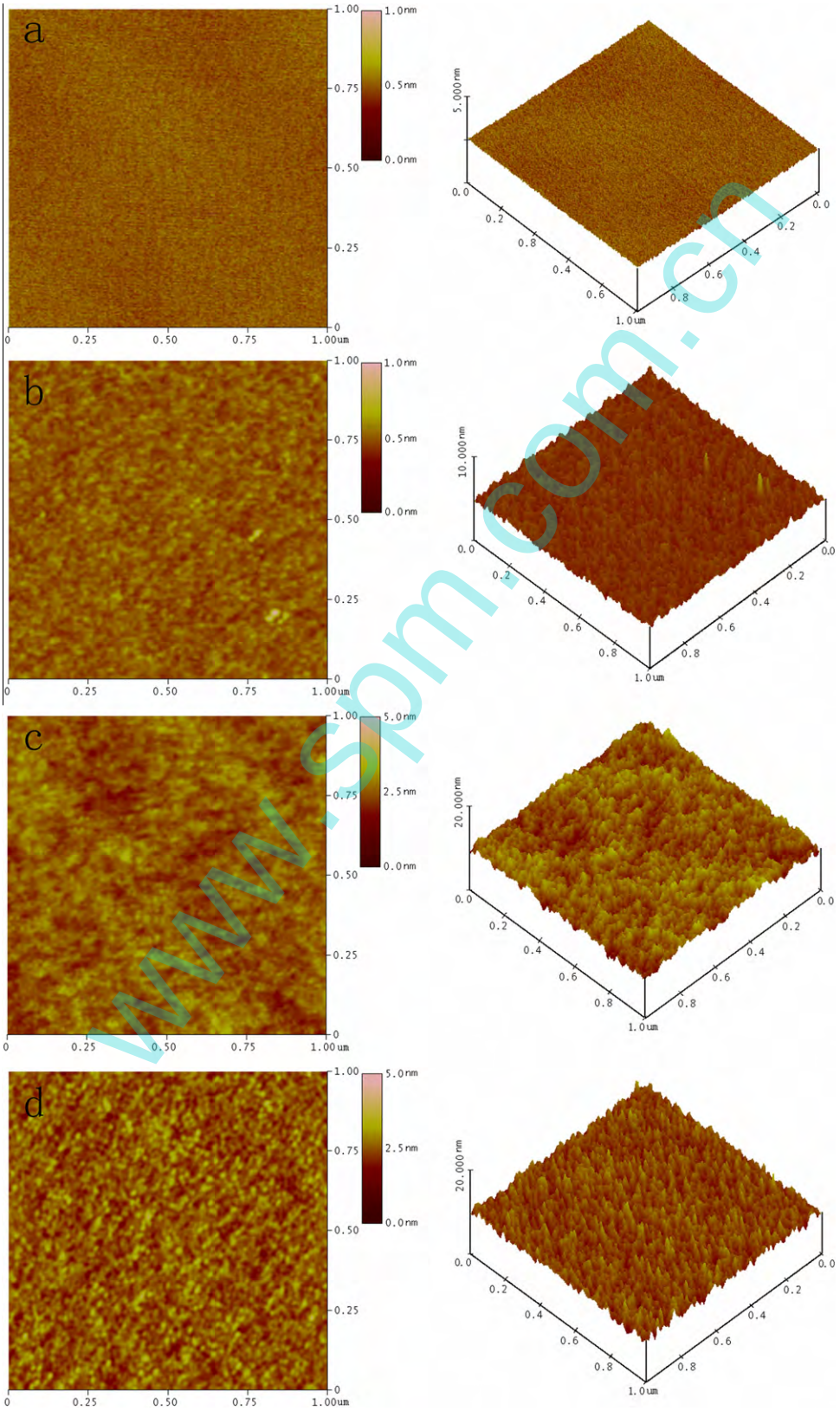

Fig. 6. 2D and 3D AFM images of various surface over a scanning range of 1 μm × 1 μm: (a) hydroxylated silicon substrate; (b) APS-SAM; (c) IL-COOH; (d) APSIL.

in a chemical shift of 1.0 eV [47,54]. As to the peak at 402.3 eV, it might come from the oxidation of some amino groups in APS [56].

To obtain the microstructure information of the thin films, AFM was used for the surface observation. 2D and 3D AFM images in Fig. 6a and b show that the hydroxylated silicon surface and APS-SAM surface are all very smooth and uniform with RMS roughness of 0.1 nm and 0.2 nm over a scanning range of 1 μm × 1 μm, respectively, while uneven large aggregates are observed on IL-COOH film surface with large RMS roughness of 0.6 nm, as shown in Fig. 6c. The surface topography of APSIL film (Fig. 6d) displays a medium roughness of about 0.4 nm, which indicates that the heat treatment improves distribution of IL-COOH molecules on APS-SAM by chemical bonding process.

3.2. Adhesive and nanotribological behaviors

Histogram of the adhesive forces between the microsphere and various films is shown in Fig. 7. Strong adhesive force of 688 nN is observed on IL-COOH film at a relative humidity of 15%. While for APSIL film, low adhesive force of 504 nN can be partially attributed to less mobile IL-COOH molecules which make it more difficult to form a meniscus than IL-COOH film. Furthermore, because micro adhesion is mainly dominated by the capillary force of water molecules adsorbed on surface [57], the adhesive forces of the thin films are related to their water contact angles (Table 1) which reflect capability of adsorbing water molecules. An exception is APS-SAM because smaller surface roughness result in a larger contact area between the microsphere and APS-SAM surface [58].

The nanotribological behaviors of the thin films investigated by the method of linearly increasing load are showed in Fig. 8. The slope of the force curve is regarded as the nominal friction coefficient (NFC) [59]. It is shown that both APSIL and IL-COOH films decrease NFC compared to APS-SAM, which indicate that a few mobile IL-COOH molecules facilitate sliding of microsphere of the colloidal probe on the surface [29]. It is well known that adhesion produced primarily by meniscus resulting from both adsorbed

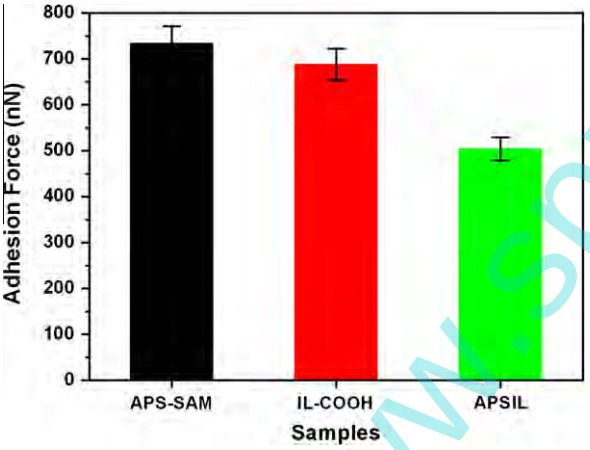

Fig. 7. Adhesive forces on APS-SAM, IL-COOH and APSIL.

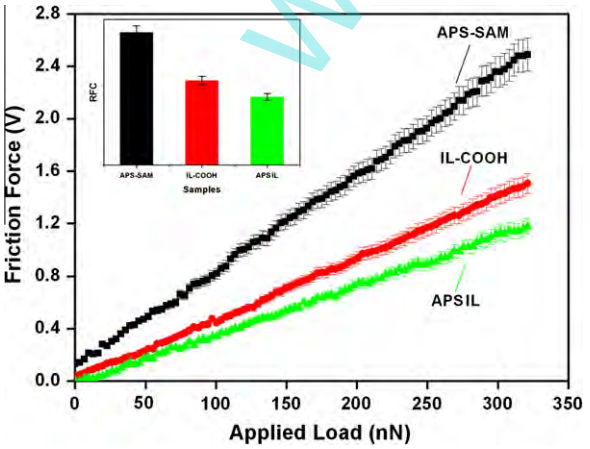

Fig. 8. Friction force versus load curves and nominal friction coefficient for APS-SAM, IL-COOH and APSIL.

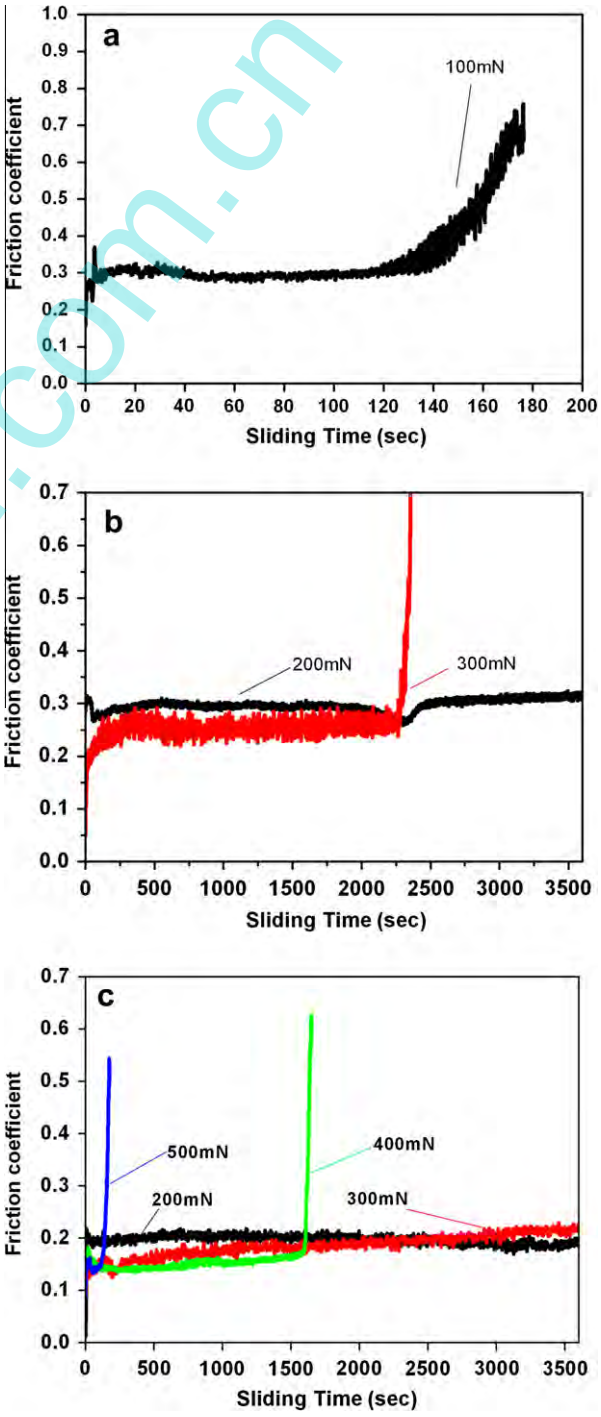

Fig. 9. Variation in friction coefficient with sliding time for various films at sliding frequency of 1 Hz: (a) APS-SAM; (b) IL-COOH film; (c) APSIL film.

water and excess mobile lubricant molecules provides greater resistance to microsphere sliding and leads to high friction coefficient at nano-scale [29,60,61]. Therefore, the dual-layer APSIL film with two-phase structure exhibits best lubricity among the three films, which can be attributed to the low adhesive force of APSIL film due to fewer mobile molecules than IL-COOH film. For IL-COOH film, due to the lack of chemical bonding, the interaction between IL-COOH molecules and the silicon substrate is weak and dewetting could occur, when the microsphere approaches the silicon surface, water and IL-COOH molecules are more likely to form a meniscus and produce large adhesive force. On the other hand, the low friction coefficient of APSIL film also can be ascribed to the outward non-polar substituted alkyl chains of bonded IL-COOH molecules possessing weaker interaction with microsphere during sliding [59], as well as having a significant freedom to swing and reorient along the sliding direction under shear stress, and consequently yielding a smaller resistance [62].

3.3. Microtribological behavior

The microtribological performances of the thin films are shown in Fig. 9, APS-SAM exhibits poor tribological properties characterized by high friction coefficient of 0.3 and very short antiwear life of 140 s under a relative mild condition (load of 100 mN, sliding frequency of 1 Hz). The poor tribological performance of APS-SAM is accord with the literature [9]. The friction coefficient versus sliding time curve for IL-COOH film is shown in Fig. 9b for comparison. It is observed that the friction coefficient of IL-COOH film kept at a high value (0.3) at load of 200 mN. When the applied normal load rises to 300 mN, the friction coefficient of IL-COOH film rises sharply over 0.6 after 2280 s and fails rapidly. As comparison with APS-SAM and IL-COOH film, the dual-layer APSIL film displays improved tribological properties (Fig. 9c), i.e., a reducing friction coefficient lower than 0.2 at all applied loads, and a extending antiwear life over 3600 s at load of 300 mN. Meanwhile, the antiwear lives of both APSIL and IL-COOH films are decreased dramatically with increasing load, which can be reasonably understood as high load would intensify the distortion of the organic molecules and accelerate the formation of defects. The gradual decrease of friction coefficient with increasing load can be explained sufficiently by Amontons' law.

To further compare the tribological behaviors between IL-COOH film and APSIL film, images of the worn surfaces for the two kinds of films are shown in Fig. 10. A very deep wear scar appears on the silicon wafer coated with IL-COOH film when the film fails at load of 300 mN (Fig. 10a). However, for silicon wafer coated with APSIL film, as shown in Fig. 10c, there is nearly no visible wear scar at load of 300 mN after sliding for 3600 s. When applied load rises to 400 mN, Fig. 10d shows that the worn surface of APSIL film exhibits slight wear when the film fails, whereas the IL-COOH film (Fig. 10b) has been deeply scratched for same sliding time of 1594 s. The results indicate that synergic effect of the steady bonded phase and flowable mobile phase for APSIL duly-layer film can reduce wear.

By analysing above experimental results, we can conclude that the significant decrease in the friction coefficient of APSIL film might be attributed to the combination of the mobile phase and bonded phase, as schematized in Fig. 3. When the steel ball counterpart squeezes mobile phase out, there is no direct contact between the steel ball and silicon substrate due to protection of bonded phase and transferred film on the steel ball counterpart. On the other hand, It can also been understood that the more densely packed and ordered dual-layer structure of APSIL film can compensate defects of the film itself and reduce friction. However, for IL-COOH film, the contact between micro-asperities of the steel ball and silicon substrate occurs frequently during sliding because there is no protection of bonded phase, which causes high friction coefficient and large fluctuation of friction coefficient. The high

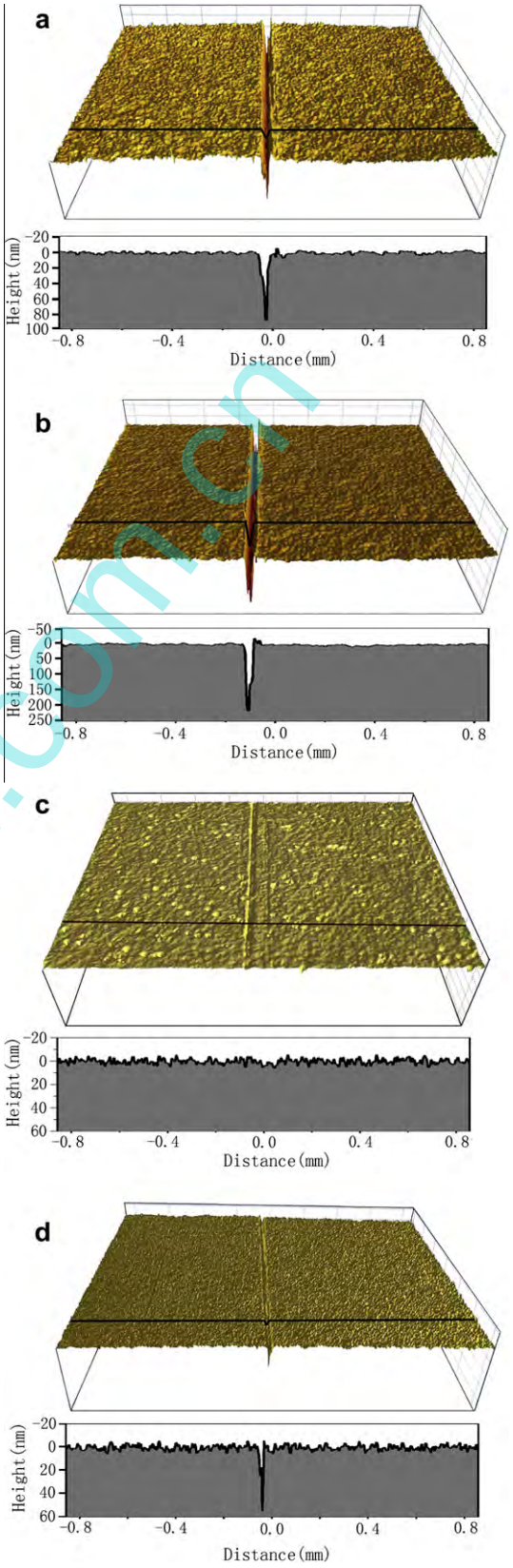

Fig. 10. Images and profile traces of the worn surfaces when the films fails at sliding frequency of 1 Hz: (a) IL-COOH film at load of 300 mN; (b) IL-COOH film at load of 400 mN for same sliding time with panel d; (c) APSIL at load of 300 mN; (d) APSIL at load of 400 mN.

antiwear and load-carrying capacities might result from the several factors. First, for the dual-layer APSIL film, the strong adhesion between the immobile layers and to silicon substrate is achieved by chemical bonding rather than physical adsorption, which is beneficial to improving the stability and load-carrying capacity of the film. In addition, interlinked hydrogen bonds among the molecules further strengthen the bonded phase of the dual-layer film. Second, the mobile phase of the dual-layer film can reorganize themselves into the original state after being mechanically disrupted during sliding, namely, a self-replenishment property. The self-replenishment phenomenon can be well observed from the morphology of worn surfaces, Fig. 10c shows that the mobile molecules replenish the wear trench. Meanwhile, a few unbonded IL-COOH molecules embed in gaps between bonded IL-COOH molecules, which makes it difficult to peeled these mobile molecules off. Third, the bonded phase of the dual-layer film possesses higher flexibility to endure larger stress and can absorb energy generated by large compression and shear during sliding against steel ball counterpart [40].

As reported by many studies, the ILs themselves showed a good prospect as lubricants for their good friction reducing and antiwear performances. The present dual-layer APSIL film, which contains both mobile and bonded phases, exhibits better tribological properties than the single-layer IL-COOH film only possessing single phase and might have promising application in the lubrication of M/NEMS.

4. Conclusions

A novel dual-layer APSIL film which contained both bonded and mobile phases in IL-COOH layer was formed on a silicon substrate by a two-step self-assembly process. The formation of a covalent amide bond was confirmed by ATR-FTIR and XPS spectra, which showed that the IL-COOH molecules were successfully grafted on APS-SAM, and hydrogen bonds existed in the molecules. The relationship between the tribological behaviors and unique structure of the APSIL film is also drawn as follows:

(1) The bonded phase of IL-COOH layer is fixed on silicon substrate by means of chemical bonding with APS anchor layer, which enhances the stability, uniformity and antiwear property of the film. The synergic effect between flowable mobile phase and steady bonded phase plays a significant role in further improving tribological properties of the film.
(2) Compared with the single-layer IL-COOH film possessing potential lubricity, the decreasing nanofriction coefficient of the as-prepared dual-layer film can be attributed to low adhesion due to fewer mobile molecules and weaker interaction between microsphere and the thin film. In addition, the presence of protective bonded phase, as well as the more densely packed and ordered layered structure, would contribute to the decrease of microfriction coefficient of the dual-layer film.
(3) The improved durability of APSIL film is related to self-replenishment property of mobile phase and enhanced load-carrying capacity of bonded phase which is strengthened by interlayer chemical bonds and interlinked hydrogen bonds.

Acknowledgments

The authors are grateful to the financial support from the Natural Science Foundation of China (Grant No. 20773148) and National 973 Program (Grant No. 2007CB607601).

References

[1] S.M. Spearing, Acta Mater. 48 (2000) 179–196.
[2] R. Yakimova, R.M. Petoral, G.R. Yazdi, C. Vahlberg, A.L. Petz, K. Uvdal, J. Phys. D: Appl. Phys. 40 (2007) 6435–6442.
[3] M. Li, H.X. Tang, M.L. Roukes, Nat. Nanotechnol. 2 (2007) 114–120.
[4] B. Bhushan, Springer Handbook of Nanotechnology, Springer-Verlag, Heidelberg, Germany, 2004.
[5] S.M. Hsu, Tribol. Int. 37 (2004) 537–545.
[6] H. Liu, B. Bhushan, Ultramicroscopy 91 (2002) 185–202.
[7] A. Ulman, Chem. Rev. 96 (1996) 1533–1554.
[8] V.V. Tsukruk, Adv. Mater. 13 (2001) 95–108.
[9] S.L. Ren, S.R. Yang, Y.P. Zhao, Langmuir 19 (2003) 2763–2767.
[10] C.D. Lorenz, M. Chandross, G.S. Grest, M.J. Stevens, E.B. Webb, Langmuir 21 (2005) 11744–11748.
[11] J. Ruhe, V.J. Novotny, K.K. Kanazawa, T. Clarke, G.B. Street, Langmuir 9 (1993) 2383–2388.
[12] J.S. Wilkes, Green Chem. 4 (2002) 73–80.
[13] T. Welton, Chem. Rev. 99 (1999) 2071–2084.
[14] K.R. Seddon, Nat. Mater. 2 (2003) 363–365.
[15] M.J. Earle, J. Esperanca, M.A. Gilea, J.N.C. Lopes, L.P.N. Rebelo, J.W. Magee, K.R. Seddon, J.A. Widegren, Nature 439 (2006) 831–834.
[16] J. Dupont, R.F. Souza, P.A.Z. Suarez, Chem. Rev. 102 (2002) 3667–3692.
[17] L. Crowhurst, N.L. Lancaster, J.M. Perez-Arlandis, T. Welton, ACS Symp. Ser. 902 (2005) 218–232.
[18] C. Kolbeck, M. Killian, F. Maier, N. Paape, P. Wasserscheid, H.P. Steinrck, Langmuir 24 (2008) 9500–9507.
[19] X.X. Han, D.W. Armstrong, Acc. Chem. Res. 40 (2007) 1079–1086.
[20] P. Wasserscheid, W. Keim, Angew. Chem., Int. Ed. 39 (2000) 3772–3789.
[21] M. Palacio, B. Bhushan, Adv. Mater 20 (2008) 1194–1198.
[22] F. Zhou, Y.M. Liang, W.M. Liu, Chem. Soc. Rev. 38 (2009) 2590–2599.
[23] C.F. Ye, W.M. Liu, Y.X. Chen, L.G. Yu, Chem. Commun. 21 (2001) 2244–2245.
[24] C.M. Jin, C.F. Ye, B.S. Phillips, J.S. Zabinski, X.Q. Liu, W.M. Liu, J.M. Shreeve, J. Mater. Chem. 16 (2006) 1529–1535.
[25] W.M. Liu, C.F. Ye, Q.Y. Gong, H.Z. Wang, P. Wang, Tribol. Lett. 13 (2002) 81–85.
[26] H.Z. Wang, Q.M. Lu, C.F. Ye, W.M. Liu, Z.J. Cui, Wear 256 (2004) 44–48.
[27] M.H. Yao, Y.M. Liang, Y.Q. Xia, F. Zhou, ACS Appl. Mater. Interfaces 1 (2009) 467–471.
[28] Z. Zeng, B.S. Phillips, J.C. Xiao, J.M. Shreeve, Chem. Mater. 20 (2008) 2719–2726.
[29] M. Forsyth, T.F. Kemp, P.C. Howlett, J.Z. Sun, M.E. Smith, J. Phys. Chem. C 112 (2008) 13801–13804.
[30] B.S. Phillips, R.A. Mantz, P.C. Trulove, J.S. Zabinski, ACS Symp. Ser. 901 (2005) 244–258.
[31] B. Yu, F. Zhou, Z.G. Mu, Y.M. Liang, W.M. Liu, Tribol.Int. 39 (2006) 879–887.
[32] W.Q. Jiang, B. Yu, W.M. Liu, J.C. Hao, Langmuir 23 (2007) 8549–8553.
[33] J.J. Nainaparampil, B.S. Phillips, K.C. Eapen, J.S. Zabinski, Nanotechnology 16 (2005) 2474–2481.
[34] M. Zhu, J. Yan, Y.F. Mo, M.W. Bai, Tribol. Lett. 29 (2008) 177–183.
[35] Y.F. Mo, W.J. Zhao, M. Zhu, M.W. Bai, Tribol. Lett. 32 (2008) 143–151.
[36] W.J. Zhao, Y.F. Mo, J.B. Pu, M.W. Bai, Tribol. Int. 42 (2009) 828–835.
[37] W.J. Zhao, Y. Wang, L.P. Wang, M.W. Bai, Q.J. Xue, Colloids Surf. A 361 (2010) 118–125.
[38] W.J. Zhao, M. Zhu, Y.F. Mo, M.W. Bai, Colloids Surf. A 332 (2009) 78–83.
[39] B. Bhushan, M. Palacio, B. Kinzig, J. Colloid Interface Sci. 317 (2008) 275–287.
[40] J. Choi, M. Kawaguchi, T. Kato, Tribol. Lett. 15 (2003) 353–358.
[41] O.A. Mazyar, G.K. Jennings, C. McCabe, Langmuir 25 (2009) 5103–5110.
[42] S.W. Tam-Chang, H.A. Biebuyck, G.M. Whitesides, N. Jeon, R.G. Nuzzo, Langmuir 11 (1995) 4371–4382.
[43] R.S. Clegg, J.E. Hutchison, J. Am. Chem. Soc. 121 (1999) 5319–5327.
[44] R.S. Clegg, S.M. Reed, J.E. Hutchison, J. Am. Chem. Soc. 120 (1998) 2486–2487.
[45] Y.T. Tao, J. Am. Chem. Soc. 115 (1993) 4350–4358.
[46] D.F.S. Petri, G. Wenz, P. Schunk, T. Schimmel, Langmuir 15 (1999) 4520–4523.
[47] W.B. Caldwell, K. Chen, C.A. Mirkin, Langmuir 9 (1993) 1945–1947.
[48] H. Wang, S. Chen, L. Li, S. Jiang, Langmuir 21 (2005) 2633–2636.
[49] N.J. Brewer, B.D. Braker, G.J. Leggett, Langmuir 17 (2001) 1970–1974.
[50] S.Y. Song, R.Q. Chu, J.F. Zhou, S.R. Yang, J.Y. Zhang, J. Phys. Chem. C 112 (2008) 3805–3810.
[51] S.Y. Song, J.F. Zhou, M.N. Qu, S.R. Yang, J.Y. Zhang, Langmuir 24 (2008) 105–109.
[52] R.S. Clegg, J.E. Hutchison, Langmuir 12 (1996) 5239–5243.
[53] K. Nakanishi, P.H. Solomon, Infrared Absorption Spectroscopy, second ed., Holden-Day Inc., San Francisco, CA, 1977.
[54] J.J. Chance, W.C. Purdy, Langmuir 13 (1997) 4487–4489.
[55] R. Wallace, P. Chen, S. Henck, D.J. Webb, Vas. Sci. Technol. A 13 (1995) 1345–1350.
[56] S. Xiao, M. Textor, N.D. Spencer, Langmuir 14 (1998) 5507–5516.
[57] D.I. Kim, J. Grobelny, N. Pradeep, R.F. Cook, Langmuir 24 (2008) 1873–1877.
[58] K.L. Johnson, K. Kendall, A.D. Roberts, Proc. R. Soc. London A 324 (1971) 301–313.
[59] N.J. Brewer, B.D. Beaker, G.J. Leggett, Langmuir 17 (2001) 1970–1974.
[60] A. Noy, C.D. Frisbie, L.F. Rozsnyai, M.S. Wrighton, S.M. Lieber, J. Am. Chem. Soc. 117 (1995) 7943–7951.
[61] S.K. Chilamakuri, B.J. Bhushan, Appl. Phys. 86 (1999) 4649–4657.
[62] S.L. Ren, S.R. Yang, J.Q. Wang, W.M. Liu, Y.P. Zhao, Chem. Mater. 16 (2004) 428–434.